

A study of B -meson decays to $\eta_c K^*$ and $\eta_c \gamma K^{(*)}$

B. Aubert,¹ M. Bona,¹ D. Boutigny,¹ Y. Karyotakis,¹ J. P. Lees,¹ V. Poireau,¹ X. Prudent,¹ V. Tisserand,¹
 A. Zghiche,¹ J. Garra Tico,² E. Grauges,² L. Lopez,³ A. Palano,³ M. Pappagallo,³ G. Eigen,⁴ B. Stugu,⁴
 L. Sun,⁴ G. S. Abrams,⁵ M. Battaglia,⁵ D. N. Brown,⁵ J. Button-Shafer,⁵ R. N. Cahn,⁵ Y. Groyzman,⁵
 R. G. Jacobsen,⁵ J. A. Kadyk,⁵ L. T. Kerth,⁵ Yu. G. Kolomensky,⁵ G. Kukartsev,⁵ D. Lopes Pegna,⁵ G. Lynch,⁵
 L. M. Mir,⁵ T. J. Orimoto,⁵ I. L. Osipenko,⁵ M. T. Ronan,^{5,*} K. Tackmann,⁵ T. Tanabe,⁵ W. A. Wenzel,⁵
 P. del Amo Sanchez,⁶ C. M. Hawkes,⁶ A. T. Watson,⁶ T. Held,⁷ H. Koch,⁷ M. Pelizaeus,⁷ T. Schroeder,⁷
 M. Steinke,⁷ D. Walker,⁸ D. J. Asgeirsson,⁹ T. Cuhadar-Donszelmann,⁹ B. G. Fulsom,⁹ C. Hearty,⁹ T. S. Mattison,⁹
 J. A. McKenna,⁹ A. Khan,¹⁰ M. Saleem,¹⁰ L. Teodorescu,¹⁰ V. E. Blinov,¹¹ A. D. Bukin,¹¹ V. P. Druzhinin,¹¹
 V. B. Golubev,¹¹ A. P. Onuchin,¹¹ S. I. Serednyakov,¹¹ Yu. I. Skovpen,¹¹ E. P. Solodov,¹¹ K. Yu. Todyshev,¹¹
 M. Bondioli,¹² S. Curry,¹² I. Eschrich,¹² D. Kirkby,¹² A. J. Lankford,¹² P. Lund,¹² M. Mandelkern,¹²
 E. C. Martin,¹² D. P. Stoker,¹² S. Abachi,¹³ C. Buchanan,¹³ S. D. Foulkes,¹⁴ J. W. Gary,¹⁴ F. Liu,¹⁴ O. Long,¹⁴
 B. C. Shen,¹⁴ L. Zhang,¹⁴ H. P. Paar,¹⁵ S. Rahatlou,¹⁵ V. Sharma,¹⁵ J. W. Berryhill,¹⁶ C. Campagnari,¹⁶
 A. Cunha,¹⁶ B. Dahmes,¹⁶ T. M. Hong,¹⁶ D. Kovalskyi,¹⁶ J. D. Richman,¹⁶ T. W. Beck,¹⁷ A. M. Eisner,¹⁷
 C. J. Flacco,¹⁷ C. A. Heusch,¹⁷ J. Kroseberg,¹⁷ W. S. Lockman,¹⁷ T. Schalk,¹⁷ B. A. Schumm,¹⁷ A. Seiden,¹⁷
 M. G. Wilson,¹⁷ L. O. Winstrom,¹⁷ E. Chen,¹⁸ C. H. Cheng,¹⁸ F. Fang,¹⁸ D. G. Hitlin,¹⁸ I. Narsky,¹⁸ T. Piatenko,¹⁸
 F. C. Porter,¹⁸ R. Andreassen,¹⁹ G. Mancinelli,¹⁹ B. T. Meadows,¹⁹ K. Mishra,¹⁹ M. D. Sokoloff,¹⁹ F. Blanc,²⁰
 P. C. Bloom,²⁰ S. Chen,²⁰ W. T. Ford,²⁰ J. F. Hirschauer,²⁰ A. Kreisel,²⁰ M. Nagel,²⁰ U. Nauenberg,²⁰ A. Olivas,²⁰
 J. G. Smith,²⁰ K. A. Ulmer,²⁰ S. R. Wagner,²⁰ J. Zhang,²⁰ A. M. Gabareen,²¹ A. Soffer,^{21,†} W. H. Toki,²¹
 R. J. Wilson,²¹ F. Winklmeier,²¹ D. D. Altenburg,²² E. Feltresi,²² A. Hauke,²² H. Jasper,²² J. Merkel,²²
 A. Petzold,²² B. Spaan,²² K. Wacker,²² V. Klose,²³ M. J. Kobel,²³ H. M. Lacker,²³ W. F. Mader,²³ R. Nogowski,²³
 J. Schubert,²³ K. R. Schubert,²³ R. Schwierz,²³ J. E. Sundermann,²³ A. Volk,²³ D. Bernard,²⁴ G. R. Bonneaud,²⁴
 E. Latour,²⁴ V. Lombardo,²⁴ Ch. Thiebaux,²⁴ M. Verderi,²⁴ P. J. Clark,²⁵ W. Gradl,²⁵ F. Muheim,²⁵ S. Playfer,²⁵
 A. I. Robertson,²⁵ J. E. Watson,²⁵ Y. Xie,²⁵ M. Andreotti,²⁶ D. Bettoni,²⁶ C. Bozzi,²⁶ R. Calabrese,²⁶ A. Cecchi,²⁶
 G. Cibinetto,²⁶ P. Franchini,²⁶ E. Luppi,²⁶ M. Negrini,²⁶ A. Petrella,²⁶ L. Piemontese,²⁶ E. Prencipe,²⁶
 V. Santoro,²⁶ F. Anulli,²⁷ R. Baldini-Ferrolì,²⁷ A. Calcaterra,²⁷ R. de Sangro,²⁷ G. Finocchiaro,²⁷ S. Pacetti,²⁷
 P. Patteri,²⁷ I. M. Peruzzi,^{27,‡} M. Piccolo,²⁷ M. Rama,²⁷ A. Zallo,²⁷ A. Buzzo,²⁸ R. Contri,²⁸ M. Lo Vetere,²⁸
 M. M. Macri,²⁸ M. R. Monge,²⁸ S. Passaggio,²⁸ C. Patrignani,²⁸ E. Robutti,²⁸ A. Santroni,²⁸ S. Tosi,²⁸
 K. S. Chaisanguanthum,²⁹ M. Morii,²⁹ J. Wu,²⁹ R. S. Dubitzky,³⁰ J. Marks,³⁰ S. Schenk,³⁰ U. Uwer,³⁰ D. J. Bard,³¹
 P. D. Dauncey,³¹ R. L. Flack,³¹ J. A. Nash,³¹ W. Panduro Vazquez,³¹ M. Tibbetts,³¹ P. K. Behera,³² X. Chai,³²
 M. J. Charles,³² U. Mallik,³² V. Ziegler,³² J. Cochran,³³ H. B. Crawley,³³ L. Dong,³³ V. Eyges,³³ W. T. Meyer,³³
 S. Prell,³³ E. I. Rosenberg,³³ A. E. Rubin,³³ Y. Y. Gao,³⁴ A. V. Gritsan,³⁴ Z. J. Guo,³⁴ C. K. Lae,³⁴ A. G. Denig,³⁵
 M. Fritsch,³⁵ G. Schott,³⁵ N. Arnaud,³⁶ J. Béquilleux,³⁶ A. D'Orazio,³⁶ M. Davier,³⁶ G. Grosdidier,³⁶ A. Höcker,³⁶
 V. Lepeltier,³⁶ F. Le Diberder,³⁶ A. M. Lutz,³⁶ S. Pruvot,³⁶ S. Rodier,³⁶ P. Roudeau,³⁶ M. H. Schune,³⁶
 J. Serrano,³⁶ V. Sordini,³⁶ A. Stocchi,³⁶ W. F. Wang,³⁶ G. Wormser,³⁶ D. J. Lange,³⁷ D. M. Wright,³⁷
 I. Bingham,³⁸ C. A. Chavez,³⁸ I. J. Forster,³⁸ J. R. Fry,³⁸ E. Gabathuler,³⁸ R. Gamet,³⁸ D. E. Hutchcroft,³⁸
 D. J. Payne,³⁸ K. C. Schofield,³⁸ C. Touramanis,³⁸ A. J. Bevan,³⁹ K. A. George,³⁹ F. Di Lodovico,³⁹ W. Menges,³⁹
 R. Sacco,³⁹ G. Cowan,⁴⁰ H. U. Flaecher,⁴⁰ D. A. Hopkins,⁴⁰ S. Paramesvaran,⁴⁰ F. Salvatore,⁴⁰ A. C. Wren,⁴⁰
 D. N. Brown,⁴¹ C. L. Davis,⁴¹ J. Allison,⁴² N. R. Barlow,⁴² R. J. Barlow,⁴² Y. M. Chia,⁴² C. L. Edgar,⁴²
 G. D. Lafferty,⁴² T. J. West,⁴² J. I. Yi,⁴² J. Anderson,⁴³ C. Chen,⁴³ A. Jawahery,⁴³ D. A. Roberts,⁴³ G. Simi,⁴³
 J. M. Tuggle,⁴³ G. Blaylock,⁴⁴ C. Dallapiccola,⁴⁴ S. S. Hertzbach,⁴⁴ X. Li,⁴⁴ T. B. Moore,⁴⁴ E. Salvati,⁴⁴
 S. Saremi,⁴⁴ R. Cowan,⁴⁵ D. Dujmic,⁴⁵ P. H. Fisher,⁴⁵ K. Koeneke,⁴⁵ G. Sciolla,⁴⁵ S. J. Sekula,⁴⁵ M. Spitznagel,⁴⁵
 F. Taylor,⁴⁵ R. K. Yamamoto,⁴⁵ M. Zhao,⁴⁵ Y. Zheng,⁴⁵ S. E. Mclachlin,^{46,*} P. M. Patel,⁴⁶ S. H. Robertson,⁴⁶
 A. Lazzaro,⁴⁷ F. Palombo,⁴⁷ J. M. Bauer,⁴⁸ L. Cremaldi,⁴⁸ V. Eschenburg,⁴⁸ R. Godang,⁴⁸ R. Kroeger,⁴⁸
 D. A. Sanders,⁴⁸ D. J. Summers,⁴⁸ H. W. Zhao,⁴⁸ S. Brunet,⁴⁹ D. Côté,⁴⁹ M. Simard,⁴⁹ P. Taras,⁴⁹ F. B. Viaud,⁴⁹
 H. Nicholson,⁵⁰ G. De Nardo,⁵¹ F. Fabozzi,^{51,§} L. Lista,⁵¹ D. Monorchio,⁵¹ C. Sciacca,⁵¹ M. A. Baak,⁵² G. Raven,⁵²
 H. L. Snoek,⁵² C. P. Jessop,⁵³ K. J. Knoepfel,⁵³ J. M. LoSecco,⁵³ G. Benelli,⁵⁴ L. A. Corwin,⁵⁴ K. Honscheid,⁵⁴

H. Kagan,⁵⁴ R. Kass,⁵⁴ J. P. Morris,⁵⁴ A. M. Rahimi,⁵⁴ J. J. Regensburger,⁵⁴ Q. K. Wong,⁵⁴ N. L. Blount,⁵⁵ J. Brau,⁵⁵ R. Frey,⁵⁵ O. Igonkina,⁵⁵ J. A. Kolb,⁵⁵ M. Lu,⁵⁵ R. Rahmat,⁵⁵ N. B. Sinev,⁵⁵ D. Strom,⁵⁵ J. Strube,⁵⁵ E. Torrence,⁵⁵ N. Gagliardi,⁵⁶ A. Gaz,⁵⁶ M. Margoni,⁵⁶ M. Morandin,⁵⁶ A. Pompili,⁵⁶ M. Posocco,⁵⁶ M. Rotondo,⁵⁶ F. Simonetto,⁵⁶ R. Stroili,⁵⁶ C. Voci,⁵⁶ E. Ben-Haim,⁵⁷ H. Briand,⁵⁷ G. Calderini,⁵⁷ J. Chauveau,⁵⁷ P. David,⁵⁷ L. Del Buono,⁵⁷ Ch. de la Vaissière,⁵⁷ O. Hamon,⁵⁷ Ph. Leruste,⁵⁷ J. Malclès,⁵⁷ J. Ocariz,⁵⁷ A. Perez,⁵⁷ J. Prendki,⁵⁷ L. Gladney,⁵⁸ M. Biasini,⁵⁹ R. Covarelli,⁵⁹ E. Manoni,⁵⁹ C. Angelini,⁶⁰ G. Batignani,⁶⁰ S. Bettarini,⁶⁰ M. Carpinelli,⁶⁰ R. Cenci,⁶⁰ A. Cervelli,⁶⁰ F. Forti,⁶⁰ M. A. Giorgi,⁶⁰ A. Lusiani,⁶⁰ G. Marchiori,⁶⁰ M. A. Mazur,⁶⁰ M. Morganti,⁶⁰ N. Neri,⁶⁰ E. Paoloni,⁶⁰ G. Rizzo,⁶⁰ J. J. Walsh,⁶⁰ M. Haire,⁶¹ J. Biesiada,⁶² P. Elmer,⁶² Y. P. Lau,⁶² C. Lu,⁶² J. Olsen,⁶² A. J. S. Smith,⁶² A. V. Telnov,⁶² E. Baracchini,⁶³ F. Bellini,⁶³ G. Cavoto,⁶³ D. del Re,⁶³ E. Di Marco,⁶³ R. Faccini,⁶³ F. Ferrarotto,⁶³ F. Ferroni,⁶³ M. Gaspero,⁶³ P. D. Jackson,⁶³ L. Li Gioi,⁶³ M. A. Mazzoni,⁶³ S. Morganti,⁶³ G. Piredda,⁶³ F. Polci,⁶³ F. Renga,⁶³ C. Voena,⁶³ M. Ebert,⁶⁴ T. Hartmann,⁶⁴ H. Schröder,⁶⁴ R. Waldi,⁶⁴ T. Adye,⁶⁵ G. Castelli,⁶⁵ B. Franek,⁶⁵ E. O. Olaiya,⁶⁵ S. Ricciardi,⁶⁵ W. Roethel,⁶⁵ F. F. Wilson,⁶⁵ S. Emery,⁶⁶ M. Escalier,⁶⁶ A. Gaidot,⁶⁶ S. F. Ganzhur,⁶⁶ G. Hamel de Monchenault,⁶⁶ W. Kozanecki,⁶⁶ G. Vasseur,⁶⁶ Ch. Yèche,⁶⁶ M. Zito,⁶⁶ X. R. Chen,⁶⁷ H. Liu,⁶⁷ W. Park,⁶⁷ M. V. Purohit,⁶⁷ J. R. Wilson,⁶⁷ M. T. Allen,⁶⁸ D. Aston,⁶⁸ R. Bartoldus,⁶⁸ P. Bechtel,⁶⁸ N. Berger,⁶⁸ R. Claus,⁶⁸ J. P. Coleman,⁶⁸ M. R. Convery,⁶⁸ J. C. Dingfelder,⁶⁸ J. Dorfan,⁶⁸ G. P. Dubois-Felsmann,⁶⁸ W. Dunwoodie,⁶⁸ R. C. Field,⁶⁸ T. Glanzman,⁶⁸ S. J. Gowdy,⁶⁸ M. T. Graham,⁶⁸ P. Grenier,⁶⁸ C. Hast,⁶⁸ T. Hryn'ova,⁶⁸ W. R. Innes,⁶⁸ J. Kaminski,⁶⁸ M. H. Kelsey,⁶⁸ H. Kim,⁶⁸ P. Kim,⁶⁸ M. L. Kocian,⁶⁸ D. W. G. S. Leith,⁶⁸ S. Li,⁶⁸ S. Luitz,⁶⁸ V. Luth,⁶⁸ H. L. Lynch,⁶⁸ D. B. MacFarlane,⁶⁸ H. Marsiske,⁶⁸ R. Messner,⁶⁸ D. R. Muller,⁶⁸ C. P. O'Grady,⁶⁸ I. Ofte,⁶⁸ A. Perazzo,⁶⁸ M. Perl,⁶⁸ T. Pulliam,⁶⁸ B. N. Ratcliff,⁶⁸ A. Roodman,⁶⁸ A. A. Salnikov,⁶⁸ R. H. Schindler,⁶⁸ J. Schwiening,⁶⁸ A. Snyder,⁶⁸ J. Stelzer,⁶⁸ D. Su,⁶⁸ M. K. Sullivan,⁶⁸ K. Suzuki,⁶⁸ S. K. Swain,⁶⁸ J. M. Thompson,⁶⁸ J. Va'vra,⁶⁸ N. van Bakel,⁶⁸ A. P. Wagner,⁶⁸ M. Weaver,⁶⁸ W. J. Wisniewski,⁶⁸ M. Wittgen,⁶⁸ D. H. Wright,⁶⁸ A. K. Yarritu,⁶⁸ K. Yi,⁶⁸ C. C. Young,⁶⁸ P. R. Burchat,⁶⁹ A. J. Edwards,⁶⁹ S. A. Majewski,⁶⁹ B. A. Petersen,⁶⁹ L. Wilden,⁶⁹ S. Ahmed,⁷⁰ M. S. Alam,⁷⁰ R. Bula,⁷⁰ J. A. Ernst,⁷⁰ V. Jain,⁷⁰ B. Pan,⁷⁰ M. A. Saeed,⁷⁰ F. R. Wappler,⁷⁰ S. B. Zain,⁷⁰ M. Krishnamurthy,⁷¹ S. M. Spanier,⁷¹ R. Eckmann,⁷² J. L. Ritchie,⁷² A. M. Ruland,⁷² C. J. Schilling,⁷² R. F. Schwitters,⁷² J. M. Izen,⁷³ X. C. Lou,⁷³ S. Ye,⁷³ F. Bianchi,⁷⁴ F. Gallo,⁷⁴ D. Gamba,⁷⁴ M. Pelliccioni,⁷⁴ M. Bomben,⁷⁵ L. Bosisio,⁷⁵ C. Cartaro,⁷⁵ F. Cossutti,⁷⁵ G. Della Ricca,⁷⁵ L. Lancieri,⁷⁵ L. Vitale,⁷⁵ V. Azzolini,⁷⁶ N. Lopez-March,⁷⁶ F. Martinez-Vidal,⁷⁶ D. A. Milanes,⁷⁶ A. Oyanguren,⁷⁶ J. Albert,⁷⁷ Sw. Banerjee,⁷⁷ B. Bhuyan,⁷⁷ K. Hamano,⁷⁷ R. Kowalewski,⁷⁷ I. M. Nugent,⁷⁷ J. M. Roney,⁷⁷ R. J. Sobie,⁷⁷ P. F. Harrison,⁷⁸ J. Ilic,⁷⁸ T. E. Latham,⁷⁸ G. B. Mohanty,⁷⁸ H. R. Band,⁷⁹ X. Chen,⁷⁹ S. Dasu,⁷⁹ K. T. Flood,⁷⁹ J. J. Hollar,⁷⁹ P. E. Kutter,⁷⁹ Y. Pan,⁷⁹ M. Pierini,⁷⁹ R. Prepost,⁷⁹ S. L. Wu,⁷⁹ and H. Neal⁸⁰

(The BABAR Collaboration)

¹Laboratoire de Physique des Particules, IN2P3/CNRS et Université de Savoie, F-74941 Annecy-Le-Vieux, France

²Universitat de Barcelona, Facultat de Física, Departament ECM, E-08028 Barcelona, Spain

³Università di Bari, Dipartimento di Fisica and INFN, I-70126 Bari, Italy

⁴University of Bergen, Institute of Physics, N-5007 Bergen, Norway

⁵Lawrence Berkeley National Laboratory and University of California, Berkeley, California 94720, USA

⁶University of Birmingham, Birmingham, B15 2TT, United Kingdom

⁷Ruhr Universität Bochum, Institut für Experimentalphysik 1, D-44780 Bochum, Germany

⁸University of Bristol, Bristol BS8 1TL, United Kingdom

⁹University of British Columbia, Vancouver, British Columbia, Canada V6T 1Z1

¹⁰Brunel University, Uxbridge, Middlesex UB8 3PH, United Kingdom

¹¹Budker Institute of Nuclear Physics, Novosibirsk 630090, Russia

¹²University of California at Irvine, Irvine, California 92697, USA

¹³University of California at Los Angeles, Los Angeles, California 90024, USA

¹⁴University of California at Riverside, Riverside, California 92521, USA

¹⁵University of California at San Diego, La Jolla, California 92093, USA

¹⁶University of California at Santa Barbara, Santa Barbara, California 93106, USA

¹⁷University of California at Santa Cruz, Institute for Particle Physics, Santa Cruz, California 95064, USA

¹⁸California Institute of Technology, Pasadena, California 91125, USA

¹⁹University of Cincinnati, Cincinnati, Ohio 45221, USA

²⁰University of Colorado, Boulder, Colorado 80309, USA

²¹Colorado State University, Fort Collins, Colorado 80523, USA

²²Universität Dortmund, Institut für Physik, D-44221 Dortmund, Germany

²³Technische Universität Dresden, Institut für Kern- und Teilchenphysik, D-01062 Dresden, Germany

²⁴Laboratoire Leprince-Ringuet, CNRS/IN2P3, Ecole Polytechnique, F-91128 Palaiseau, France

- ²⁵University of Edinburgh, Edinburgh EH9 3JZ, United Kingdom
- ²⁶Università di Ferrara, Dipartimento di Fisica and INFN, I-44100 Ferrara, Italy
- ²⁷Laboratori Nazionali di Frascati dell'INFN, I-00044 Frascati, Italy
- ²⁸Università di Genova, Dipartimento di Fisica and INFN, I-16146 Genova, Italy
- ²⁹Harvard University, Cambridge, Massachusetts 02138, USA
- ³⁰Universität Heidelberg, Physikalisches Institut, Philosophenweg 12, D-69120 Heidelberg, Germany
- ³¹Imperial College London, London, SW7 2AZ, United Kingdom
- ³²University of Iowa, Iowa City, Iowa 52242, USA
- ³³Iowa State University, Ames, Iowa 50011-3160, USA
- ³⁴Johns Hopkins University, Baltimore, Maryland 21218, USA
- ³⁵Universität Karlsruhe, Institut für Experimentelle Kernphysik, D-76021 Karlsruhe, Germany
- ³⁶Laboratoire de l'Accélérateur Linéaire, IN2P3/CNRS et Université Paris-Sud 11, Centre Scientifique d'Orsay, B. P. 34, F-91898 ORSAY Cedex, France
- ³⁷Lawrence Livermore National Laboratory, Livermore, California 94550, USA
- ³⁸University of Liverpool, Liverpool L69 7ZE, United Kingdom
- ³⁹Queen Mary, University of London, E1 4NS, United Kingdom
- ⁴⁰University of London, Royal Holloway and Bedford New College, Egham, Surrey TW20 0EX, United Kingdom
- ⁴¹University of Louisville, Louisville, Kentucky 40292, USA
- ⁴²University of Manchester, Manchester M13 9PL, United Kingdom
- ⁴³University of Maryland, College Park, Maryland 20742, USA
- ⁴⁴University of Massachusetts, Amherst, Massachusetts 01003, USA
- ⁴⁵Massachusetts Institute of Technology, Laboratory for Nuclear Science, Cambridge, Massachusetts 02139, USA
- ⁴⁶McGill University, Montréal, Québec, Canada H3A 2T8
- ⁴⁷Università di Milano, Dipartimento di Fisica and INFN, I-20133 Milano, Italy
- ⁴⁸University of Mississippi, University, Mississippi 38677, USA
- ⁴⁹Université de Montréal, Physique des Particules, Montréal, Québec, Canada H3C 3J7
- ⁵⁰Mount Holyoke College, South Hadley, Massachusetts 01075, USA
- ⁵¹Università di Napoli Federico II, Dipartimento di Scienze Fisiche and INFN, I-80126, Napoli, Italy
- ⁵²NIKHEF, National Institute for Nuclear Physics and High Energy Physics, NL-1009 DB Amsterdam, The Netherlands
- ⁵³University of Notre Dame, Notre Dame, Indiana 46556, USA
- ⁵⁴Ohio State University, Columbus, Ohio 43210, USA
- ⁵⁵University of Oregon, Eugene, Oregon 97403, USA
- ⁵⁶Università di Padova, Dipartimento di Fisica and INFN, I-35131 Padova, Italy
- ⁵⁷Laboratoire de Physique Nucléaire et de Hautes Energies, IN2P3/CNRS, Université Pierre et Marie Curie-Paris6, Université Denis Diderot-Paris7, F-75252 Paris, France
- ⁵⁸University of Pennsylvania, Philadelphia, Pennsylvania 19104, USA
- ⁵⁹Università di Perugia, Dipartimento di Fisica and INFN, I-06100 Perugia, Italy
- ⁶⁰Università di Pisa, Dipartimento di Fisica, Scuola Normale Superiore and INFN, I-56127 Pisa, Italy
- ⁶¹Prairie View A&M University, Prairie View, Texas 77446, USA
- ⁶²Princeton University, Princeton, New Jersey 08544, USA
- ⁶³Università di Roma La Sapienza, Dipartimento di Fisica and INFN, I-00185 Roma, Italy
- ⁶⁴Universität Rostock, D-18051 Rostock, Germany
- ⁶⁵Rutherford Appleton Laboratory, Chilton, Didcot, Oxon, OX11 0QX, United Kingdom
- ⁶⁶DSM/Dapnia, CEA/Saclay, F-91191 Gif-sur-Yvette, France
- ⁶⁷University of South Carolina, Columbia, South Carolina 29208, USA
- ⁶⁸Stanford Linear Accelerator Center, Stanford, California 94309, USA
- ⁶⁹Stanford University, Stanford, California 94305-4060, USA
- ⁷⁰State University of New York, Albany, New York 12222, USA
- ⁷¹University of Tennessee, Knoxville, Tennessee 37996, USA
- ⁷²University of Texas at Austin, Austin, Texas 78712, USA
- ⁷³University of Texas at Dallas, Richardson, Texas 75083, USA
- ⁷⁴Università di Torino, Dipartimento di Fisica Sperimentale and INFN, I-10125 Torino, Italy
- ⁷⁵Università di Trieste, Dipartimento di Fisica and INFN, I-34127 Trieste, Italy
- ⁷⁶IFIC, Universitat de Valencia-CSIC, E-46071 Valencia, Spain
- ⁷⁷University of Victoria, Victoria, British Columbia, Canada V8W 3P6
- ⁷⁸Department of Physics, University of Warwick, Coventry CV4 7AL, United Kingdom
- ⁷⁹University of Wisconsin, Madison, Wisconsin 53706, USA
- ⁸⁰Yale University, New Haven, Connecticut 06511, USA

(Dated: July 16, 2007)

We present preliminary results of a study of the two-body B -meson decays to a charmonium state ($c\bar{c}$) and a K^+ or $K^{*0}(892)$ meson using a sample of about 349 fb^{-1} of data collected with the BABAR detector at the PEP-II asymmetric-energy B Factory at SLAC. Here $c\bar{c}$ indicates either the η_c

state, reconstructed in the $K_S^0 K^\pm \pi^\mp$ and $K^+ K^- \pi^0$ decay channels, or the h_c state, reconstructed in its decay to $\eta_c \gamma$. We measure $\mathcal{B}(B^0 \rightarrow \eta_c K^{*0}) = (6.1 \pm 0.8_{\text{stat}} \pm 1.1_{\text{syst}}) \times 10^{-4}$, $\mathcal{B}(B^+ \rightarrow h_c K^+) \times \mathcal{B}(h_c \rightarrow \eta_c \gamma) < 5.2 \times 10^{-5}$ and $\mathcal{B}(B^0 \rightarrow h_c K^{*0}) \times \mathcal{B}(h_c \rightarrow \eta_c \gamma) < 2.41 \times 10^{-4}$, at the 90% C.L.

PACS numbers: 13.25.Gv, 13.25.Hw

The B decays to S-wave charmonium states, like J/ψ and η_c , have been observed to occur with large branching fractions (\mathcal{B}) of the order 10^{-3} [1]. Experimental study of B decays to singlet states of charmonium, such as η_c and h_c , is more complicated than the B decays to triplet states, such as J/ψ , $\psi(2S)$ or χ_{c1} , because one cannot exploit the cleaner signature of final states including a lepton pair. In this document, we report measurements of the branching fraction for the following decay modes: $B^0 \rightarrow \eta_c K^{*0}$, $B^0 \rightarrow h_c K^{*0}$ and $B^+ \rightarrow h_c K^+$ [2]. We also reconstruct the $B^+ \rightarrow \eta_c K^+$ decay to be used as a “control sample”. The branching fraction of $B^0 \rightarrow \eta_c K^{*0}$ is currently known with a 40% uncertainty, $(1.2 \pm 0.5) \times 10^{-3}$ [3], while B decays to h_c have never been observed. The Belle collaboration studied the decay $B^+ \rightarrow h_c K^+$ with $h_c \rightarrow \eta_c \gamma$ and reported $\mathcal{B}(B^+ \rightarrow \eta_c \gamma K^+) < 3.8 \times 10^{-5}$ at the 90% C.L. for an invariant mass of the $\eta_c \gamma$ pair in the range $[3.47, 3.57]$ GeV/ c^2 [4]. No other B^+ or B^0 decay modes with h_c have been studied yet. The h_c meson has recently been discovered by the CLEO collaboration as a narrow peak in $\psi(2S) \rightarrow \eta_c \gamma \pi^0$ decays at a mass of 3524.4 ± 0.7 MeV/ c^2 [5], and this observation was confirmed by the E835 collaboration [6].

In the simplest approximation, B decays to a charmonium state and a K or K^* meson arise from the quark-level process $b \rightarrow c \bar{c} s$. The colorless current $\bar{c} \gamma_\mu (1 - \gamma_5) c$, which can create the S-wave states like η_c and J/ψ , can also create the P-wave state χ_{c1} . It cannot, however, create the 0^{++} , 2^{++} and 1^{+-} states χ_{c0} , χ_{c2} and h_c . Therefore B decays to any of these three states have to be ascribed to more complex mechanisms, such as the interaction of two color-octet currents [7]. In this scenario, B decays to χ_{c0} , χ_{c2} or h_c are expected to occur as abundantly as those to χ_{c1} . B decays to $\chi_{c1} K^{(*)}$ have branching fractions between 3.2×10^{-4} and 4.9×10^{-4} [1]. The $B^+ \rightarrow \chi_{c0} K^+$ decay has indeed been observed with a branching fraction of $(1.4_{-0.19}^{+0.23}) \times 10^{-4}$ [1]. However B decays to $\chi_{c2} K^{(*)}$ and $h_c K^{(*)}$ have not yet been observed and upper limits on their branching fractions slightly exceed 10^{-5} [1].

In this analysis we reconstruct the η_c in the $K_S^0 (\rightarrow \pi^+ \pi^-) K^\pm \pi^\mp$ and $K^+ K^- \pi^0$ decay modes, the h_c in its decay to $\eta_c \gamma$, and the K^{*0} in the mode $K^{*0} \rightarrow K^+ \pi^-$. The $K_S^0 K^\pm \pi^\mp$ and $K^+ K^- \pi^0$ final states are manifestations of the same decay mode, $K \bar{K} \pi$: they are chosen because they are among the easiest η_c decay modes to reconstruct and have a rather large branching fraction, $\mathcal{B}(\eta_c \rightarrow K \bar{K} \pi) = (7.0 \pm 1.2)\%$ [1]. The $\eta_c \gamma$ decay

of the h_c is chosen because it is expected to comprise about half of the total h_c decay width [7]. We measure ratios of branching fractions with respect to that of $B^+ \rightarrow \eta_c K^+$, $(9.1 \pm 1.3) \times 10^{-4}$, to cancel the 17% uncertainty on $\mathcal{B}(\eta_c \rightarrow K \bar{K} \pi)$.

The data used in this analysis were collected with the BABAR detector at the PEP-II $e^+ e^-$ storage rings, and correspond to about 349 fb $^{-1}$ of integrated luminosity collected at the $\Upsilon(4S)$ resonance, comprising 384 million $B \bar{B}$ pairs. The BABAR detector is described elsewhere [8]. Momenta of charged particles are measured in a tracking system consisting of a five-layer, double-sided silicon vertex tracker and a 40-layer drift chamber (DCH), both in a 1.5-T solenoidal magnetic field. Identification of charged particles is provided by measurements of the energy loss in the tracking devices and by a ring-imaging Cherenkov detector. Photons are detected by a CsI(Tl) electromagnetic calorimeter (EMC). The BABAR detector Monte Carlo (MC) simulation based on GEANT4 [9] is used to determine selection criteria and efficiencies.

The event selection is optimized by maximizing the quantity $N_S / \sqrt{N_S + N_B}$, where N_S (N_B) represents the number of signal (background) candidates surviving the selection. N_S is estimated on samples of simulated events, while N_B is extrapolated from regions far from the signals on data. Simulated signal events and data are normalized to each other using the available measurements for $B \rightarrow \eta_c$ decays and assuming $\mathcal{B} = 1 \times 10^{-5}$ for B decays to h_c .

We select events with $B \bar{B}$ pairs by requiring at least four charged tracks, the ratio of the second to the zeroth order Fox-Wolfram moment [10] to be less than 0.2, and the total energy of all the charged and neutral particles to be greater than 4.5 GeV.

Charged pion and kaon candidates are reconstructed tracks having polar angles in the region $0.41 < \theta < 2.54$ rad, at least 12 hits in the DCH, a transverse momentum with respect to the beam direction larger than 100 MeV/ c , and a distance of closest approach to the beam spot smaller than 1.5 cm in the plane transverse to the beam axis and 10 cm along the beam axis. A K^{*0} candidate is formed from a pair of oppositely charged kaon and pion candidates originating from a common vertex and having an invariant mass within 60 MeV/ c^2 of the nominal K^{*0} mass [1].

Photon candidates are energy deposits in the EMC in the polar angle range $0.32 < \theta < 2.44$ rad that are not associated with charged tracks, have energy greater than 100 MeV, and have a shower shape consistent with that

of a photon. A $\pi^0 \rightarrow \gamma\gamma$ candidate is formed from a pair of photon candidates with invariant mass in the range [115,150] MeV/ c^2 and energy greater than 400 MeV. The mass of such candidates is constrained to the nominal π^0 mass [1] when subsequently computing kinematic quantities.

A $K_s^0 \rightarrow \pi^+\pi^-$ candidate is formed from a pair of oppositely-charged tracks originating from a common vertex and having an invariant mass within 20 MeV/ c^2 of the K^0 -meson mass. Its measured decay-length significance is required to exceed three standard deviations (σ). The candidate is constrained to the nominal K^0 mass [1].

The $B^{+,0} \rightarrow \eta_c K^{+,*0}$ candidates are formed by pairing a K^{*0} or K^+ candidate, referred to as the primary kaon, and a $K_s^0 K^\pm \pi^\mp$ or $K^+ K^- \pi^0$ combination with invariant mass in the range [2.75, 3.35] GeV/ c^2 . The mass range includes the J/ψ resonance. The $B^{+,0} \rightarrow \eta_c \gamma K^{+,*0}$ candidates are formed by combining a K^{*0} or K^+ candidate, a photon with energy exceeding 250 MeV, and a $K_s^0 K^\pm \pi^\mp$ or $K^+ K^- \pi^0$ combination with invariant mass consistent with the η_c mass. We perform a vertex fit to the B candidates and require the probability of the χ^2 of the fit to exceed 0.002. We define two kinematic variables: the beam-energy substituted mass, $m_{\text{ES}} = \sqrt{E_{\text{beam}}^2 - p_B^2}$ and $\Delta E = E_B - E_{\text{beam}}$, where p_B (E_B) is the reconstructed B momentum (energy) and E_{beam} the beam energy, in the e^+e^- center-of-mass (c.m.) frame. B candidates are retained if they have m_{ES} greater than 5.2 GeV/ c^2 and ΔE within [-24,30], [-40,30], [-34,30], and [-40,30] MeV for the $K_s^0 K^\pm \pi^\mp K^{*0,+}$, $K^+ K^- \pi^0 K^{*0,+}$, $K_s^0 K^\pm \pi^\mp \gamma K^{*0,+}$, and $K^+ K^- \pi^0 \gamma K^{*0,+}$ combinations, respectively. We also require the absolute value of the cosine of the polar angle of the B candidate momentum vector in the e^+e^- c.m. frame to be smaller than 0.9.

To suppress background, the $K^+\pi^-$, K^+K^- , $K^+K_s^0$ and $K^+\pi^-\pi^+$ combinations with invariant masses within 30 MeV/ c^2 of the D^0 , D_s and D^+ meson masses [1], respectively, are excluded to form B candidates. We also remove K^+K^- combinations containing a primary kaon where the invariant mass of the combination is within 30 MeV/ c^2 of the ϕ meson mass [1].

In events where more than one B candidate survives the selection, the one with the smallest $|\Delta E|$ is retained. In cases of B candidates composed by the same final state particles, thus having the same value of $|\Delta E|$, we retain the one for which the primary kaon has the largest momentum in the e^+e^- c.m. system.

The samples surviving the selection include a signal component, a combinatorial background component given by random combinations of tracks and neutral clusters both from $B\bar{B}$ and continuum events, and a component due to B decays with a similar final state as the signal. Such “peaking backgrounds” exhibit the same distribution as the signal in m_{ES} and ΔE , but their $K\bar{K}\pi(\gamma)$ invariant-mass distribution (m_X) is different. The signal content on data is therefore obtained by means of

a maximum likelihood fit to m_X for all candidates having m_{ES} in the signal region [5.274, 5.284] GeV/ c^2 , after subtracting the combinatorial background. The m_X distribution for the combinatorial background events is obtained by extrapolating into the m_{ES} signal region the m_X distribution measured in the m_{ES} sideband, defined by $m_{\text{ES}} < 5.26$ GeV/ c^2 . The correlation between m_X and m_{ES} is found to be negligible in the relevant regions. A binned fit is then performed on the m_{ES} -sideband-subtracted m_X distribution.

We perform an unbinned maximum likelihood fit to the m_{ES} distribution as follows. The B component, accounting for the sum of signal and peaking background, is modelled by a Gaussian function whose width is taken from the simulation and whose mean is fixed to the B -meson mass [1]. The m_{ES} distribution of the combinatorial background is represented by an ARGUS threshold function [11]. The total number of events and the ARGUS parameters are left free in the fit. The spectrum for candidates in the m_{ES} sideband is normalized to the m_{ES} signal window by using the integrals of the ARGUS component in the two regions (Fig. 1).

In the case of $B^0 \rightarrow \eta_c K^{*0}$, the m_{ES} -sideband-subtracted m_X distribution is fitted to the sum of an η_c signal represented by a non-relativistic Breit-Wigner convolved with a Gaussian resolution function, a J/ψ component modelled by a Gaussian of the same width, and a background component accounted for by a first-order polynomial with free coefficients. The masses of the η_c and the J/ψ are fixed to the world average [1]. The width of the η_c is fixed to the value measured by BABAR, 34.3 MeV/ c^2 [13]. The mass resolution modelled by the width of the Gaussian functions is fixed to the value determined on MC events, 11 MeV/ c^2 . The number of signal and background events is left free in the fit. We measure 185 ± 22 η_c and 59 ± 12 J/ψ candidates (Fig. 2). The χ^2 value for the fit is 54 for 56 degrees of freedom (N_{DoF}). Repeating the fit with no η_c component we get a χ^2/N_{DoF} of 127/57. A similar fit of the $B^+ \rightarrow \eta_c K^+$ control sample yields 670 ± 32 η_c and 149 ± 16 J/ψ candidates with a χ^2/N_{DoF} of 86/56. All of the values returned by these fits are summarized in Table I.

TABLE I: Number of η_c (N_{η_c}) and J/ψ ($N_{J/\psi}$) events obtained from the fits described in the text with statistical errors only.

Mode	N_{η_c}	$N_{J/\psi}$	χ^2/N_{DoF}
$B^0 \rightarrow (K\bar{K}\pi)K^{*0}$	185 ± 22	59 ± 12	54/56
$B^+ \rightarrow (K\bar{K}\pi)K^+$	670 ± 32	149 ± 16	86/56

In the case of $B^+ \rightarrow \eta_c \gamma K^+$ and $B^0 \rightarrow \eta_c \gamma K^{*0}$, the m_{ES} -sideband-subtracted m_X distribution is fitted to the sum of an h_c signal modelled by a Gaussian, and

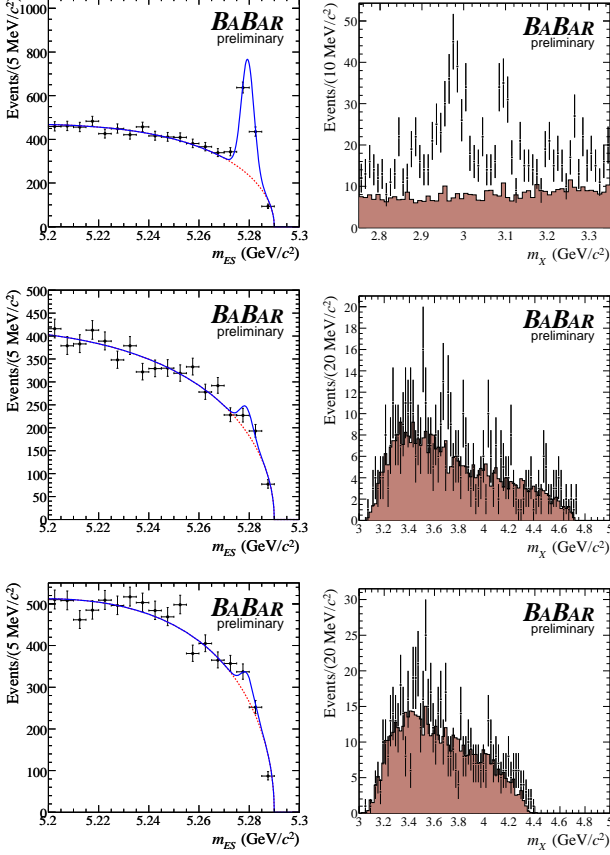


FIG. 1: Left: m_{ES} distribution for $B^0 \rightarrow (K\bar{K}\pi)K^{*0}$ (top), $B^+ \rightarrow \eta_c \gamma K^+$ (middle) and $B^0 \rightarrow \eta_c \gamma K^{*0}$ (bottom) candidates; points with error bars are data, the solid line represents the result of the fit described in the text, the dotted line represents the ARGUS component. Right: invariant mass distribution of the $K\bar{K}\pi(\gamma)$ system for $B^0 \rightarrow (K\bar{K}\pi)K^{*0}$ (top), $B^+ \rightarrow \eta_c \gamma K^+$ (middle) and $B^0 \rightarrow \eta_c \gamma K^{*0}$ (bottom) decays; points with error bars are data in the m_{ES} signal region, the shaded area represents the background expected from the m_{ES} sideband. In the top plot, η_c and J/ψ peaks are visible; peaking background events are also present as signalled by the excess of the data points above the shaded area outside the two peaks. No appreciable B component, neither signal nor peaking background, is observed for the $B^+ \rightarrow \eta_c \gamma K^+$ and $B^0 \rightarrow \eta_c \gamma K^{*0}$ cases.

a background represented by a first-order polynomial. The mass of the h_c is fixed to the CLEO measurement, 3.524 GeV/ c^2 [5]. The Gaussian resolution is fixed to the value determined on MC events, 16 MeV/ c^2 [12]. In the fit, the number of signal and background events is left free. The fit is performed over the m_X range [3.3, 3.7] GeV/ c^2 . It yields 11 ± 6 and 21 ± 8 h_c candidates with a χ^2/N_{DoF} of 41/39 and 42/39 for the B^+ and B^0 yields, respectively (Fig. 3 and Table II). Repeating these fits with no h_c component, we get a χ^2/N_{DoF} of 45/40 and 48/40.

The stability of the fit results is verified for various

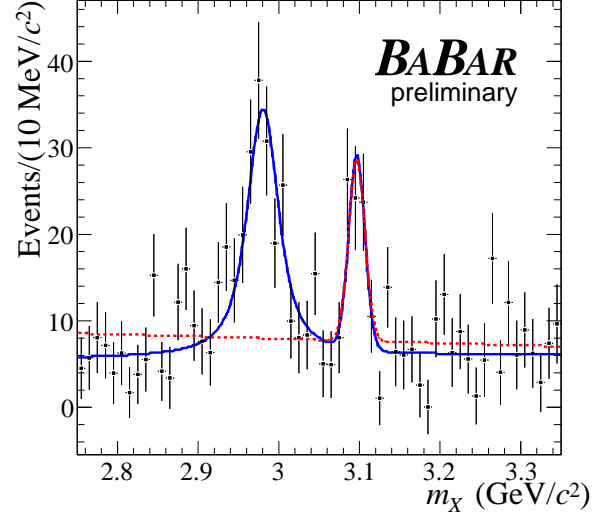


FIG. 2: Fit result (solid blue line) superimposed on the m_{ES} -sideband-subtracted m_X distribution (points with error bars) for $B^0 \rightarrow (K\bar{K}\pi)K^{*0}$. The (red) dashed line is the result of the fit with no η_c component.

TABLE II: Number of h_c (N_{h_c}) obtained from the fits described in the text with statistical errors only.

Mode	N_{h_c}	χ^2/N_{DoF}
$B^+ \rightarrow (\eta_c \gamma) K^+$	11 ± 6	41/39
$B^0 \rightarrow (\eta_c \gamma) K^{*0}$	21 ± 8	42/39

configurations of the fitting conditions. We float the η_c mass and width, which are poorly known, and the h_c mass. The values for the signal yields and the floated parameters returned by these fits are consistent with the nominal configuration. We verify the goodness of the fit with the chosen model using a MC technique: we simulate a number of experiments by randomly generating samples of events distributed in m_X according to the models used in the fit. The number of events generated is equal to the number of events in the corresponding real data sample. The parameters of the distributions are set to their fixed or fitted values. The fit is repeated in the same conditions as on real data. The pulls for the number of signal and background events are distributed as expected. The robustness of the fit is tested on simulated events by varying the number of signal and background events input, including the null result. The number of events returned by the fit is consistent with the inputs for all cases. As an additional cross-check, we verify that the observed number of J/ψ candidates in the data agrees with the expectations.

We evaluate systematic uncertainties on the number of signal candidates by individually varying the parameters

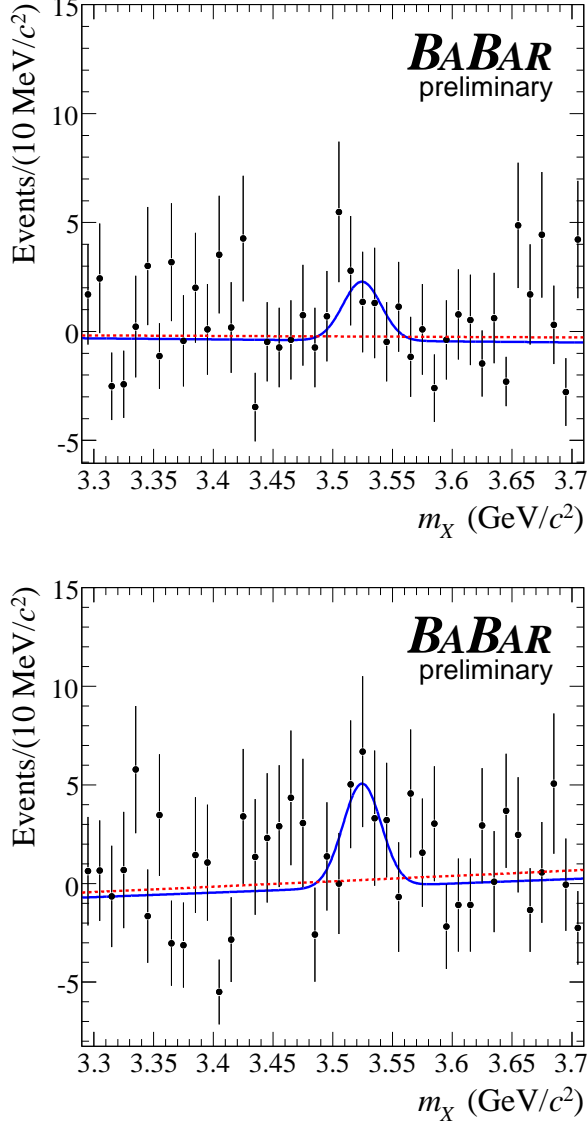


FIG. 3: Fit result (solid blue line) superimposed on the m_{ES} -sideband-subtracted m_X distribution (points with error bars) for $B^+ \rightarrow \eta_c \gamma K^+$ (top) and $B^0 \rightarrow \eta_c \gamma K^{*0}$ (bottom). No significant h_c signal is evident. The (red) dashed line is the result of the fit with no signal component.

that are fixed in the fits by $\pm 1\sigma$ from their nominal values. We also estimate the systematic uncertainties that arise from a different choice of binning, fit range, and background parameterization. The large natural width of the η_c introduces the possibility of interference effects with non-resonant B decays with the same final state particles that can modify the m_X distribution with respect to the one used in the fit. The fit is repeated including an interference term between the η_c and the background in the fitting functions. The amplitude and phase of the interference term are left free in the fit. The variation of the η_c yield with respect to the nominal fit is taken

as a conservative estimate of the systematic error due to neglecting interference effects. The total systematic uncertainty on the signal yield determination, summing in quadrature all the contributions, is 8.1, 4.3, 24.8 and 18.1% for $B^+ \rightarrow \eta_c K^+$, $B^0 \rightarrow \eta_c K^{*0}$, $B^+ \rightarrow h_c K^+$ and $B^0 \rightarrow h_c K^{*0}$, respectively. Being evaluated as yield variations on the data, most of these systematic uncertainties should improve with larger statistics.

The selection efficiency for $B^+ \rightarrow \eta_c K^+$ is 6%. The ratios of the selection efficiencies with respect to $B^+ \rightarrow \eta_c K^+$, estimated by using simulated events, are 0.64 ± 0.01 , 0.51 ± 0.01 and 0.29 ± 0.02 for $B^0 \rightarrow \eta_c K^{*0}$, $B^+ \rightarrow h_c K^+$ and $B^0 \rightarrow h_c K^{*0}$, respectively. Most uncertainties on the efficiency cancel out in the ratios because of the similar final states. The remaining uncertainties are mainly due to differences between real data and simulation in the photon reconstruction as estimated from photon control samples on data (1.8%), and the unknown polarization for $B^0 \rightarrow h_c K^{*0}$ estimated as in [14] (6%).

Using the signal efficiency computed on MC events, the signal yield observed on data, and the number of $B\bar{B}$ pairs in the data sample, we derive $\mathcal{B}(B^+ \rightarrow \eta_c K^+) \times \mathcal{B}(\eta_c \rightarrow K\bar{K}\pi) = (7.5 \pm 0.4_{\text{stat}}) \times 10^{-5}$. This is in agreement with the world average $(6.4 \pm 1.4) \times 10^{-5}$ [1].

We calculate the ratios of the branching fractions with respect to $\mathcal{B}(B^+ \rightarrow \eta_c K^+)$ using the ratios of signal yields and efficiencies with respect to $B^+ \rightarrow \eta_c K^+$, $R_\gamma = \Gamma(\Upsilon(4S) \rightarrow B^+ B^-) / \Gamma(\Upsilon(4S) \rightarrow B^0 \bar{B}^0) = 1.026 \pm 0.032$ [1], and $\mathcal{B}(K^{*0} \rightarrow K^+ \pi^-) = 2/3$, and summing the uncertainties in quadrature. Table III summarizes the systematic uncertainties on the measurements. We obtain:

$$\frac{\mathcal{B}(B^0 \rightarrow \eta_c K^{*0})}{\mathcal{B}(B^+ \rightarrow \eta_c K^+)} = 0.67 \pm 0.09_{\text{stat}} \pm 0.07_{\text{syst}},$$

and the 90% C.L. upper limits

$$\begin{aligned} \frac{\mathcal{B}(B^+ \rightarrow h_c K^+) \times \mathcal{B}(h_c \rightarrow \eta_c \gamma)}{\mathcal{B}(B^+ \rightarrow \eta_c K^+)} &< 0.058, \\ \frac{\mathcal{B}(B^0 \rightarrow h_c K^{*0}) \times \mathcal{B}(h_c \rightarrow \eta_c \gamma)}{\mathcal{B}(B^+ \rightarrow \eta_c K^+)} &< 0.26. \end{aligned}$$

These are determined assuming that the measurements follow a Gaussian distribution around the central value with standard deviation given by the total statistical plus systematic uncertainty.

Using $\mathcal{B}(B^+ \rightarrow \eta_c K^+) = (9.1 \pm 1.3) \times 10^{-4}$, we derive

$$\mathcal{B}(B^0 \rightarrow \eta_c K^{*0}) = (6.1 \pm 0.8_{\text{stat}} \pm 0.6_{\text{syst}} \pm 0.9_{\text{br}}) \times 10^{-4},$$

where the last error is from the uncertainty on $\mathcal{B}(B^+ \rightarrow \eta_c K^+)$, and the 90% C.L. upper limits

$$\begin{aligned} \mathcal{B}(B^+ \rightarrow h_c K^+) \times \mathcal{B}(h_c \rightarrow \eta_c \gamma) &< 5.2 \times 10^{-5}, \\ \mathcal{B}(B^0 \rightarrow h_c K^{*0}) \times \mathcal{B}(h_c \rightarrow \eta_c \gamma) &< 2.41 \times 10^{-4}. \end{aligned}$$

TABLE III: Summary of the relative contributions to the systematic error on $R_{\eta_c K^*} = \mathcal{B}(B^0 \rightarrow \eta_c K^{*0})/\mathcal{B}(B^+ \rightarrow \eta_c K^+)$, $R_{h_c K} = \mathcal{B}(B^+ \rightarrow h_c K^+) \times \mathcal{B}(h_c \rightarrow \eta_c \gamma)/\mathcal{B}(B^+ \rightarrow \eta_c K^+)$ and $R_{h_c K^*} = \mathcal{B}(B^0 \rightarrow h_c K^{*0}) \times \mathcal{B}(h_c \rightarrow \eta_c \gamma)/\mathcal{B}(B^+ \rightarrow \eta_c K^+)$.

	$\sigma(R)/R$ (%)		
	$R_{\eta_c K^*}$	$R_{h_c K}$	$R_{h_c K^*}$
Signal yield extraction	4.3	24.8	18.1
Signal efficiency	1.4	2.2	6.7
$\eta_c K^+$ yield extraction	8.1	8.1	8.1
R_T	3.1	—	3.1
Total	9.8	26.2	21.1

Finally, we calculate

$$\frac{\mathcal{B}(B^0 \rightarrow h_c K^{*0}) \times \mathcal{B}(h_c \rightarrow \eta_c \gamma)}{\mathcal{B}(B^0 \rightarrow \eta_c K^{*0})} < 0.39$$

at the 90% C.L.

In summary, we obtain a measurement of $\mathcal{B}(B^0 \rightarrow \eta_c K^{*0})$ in agreement with, and greatly improving upon, the previous world average. We obtain an upper limit for $\mathcal{B}(B^+ \rightarrow h_c K^+) \times \mathcal{B}(h_c \rightarrow \eta_c \gamma)$ in agreement with the result obtained by the previous Belle measurement, and a first upper limit on $\mathcal{B}(B^0 \rightarrow h_c K^{*0}) \times \mathcal{B}(h_c \rightarrow \eta_c \gamma)$. The results confirm the suppression of h_c production in B decays with respect to the S-wave η_c and the P-wave χ_{c1} and χ_{c0} states. All results are preliminary.

ACKNOWLEDGMENTS

We are grateful for the extraordinary contributions of our PEP-II colleagues in achieving the excellent luminosity and machine conditions that have made this work possible. The success of this project also relies critically on the expertise and dedication of the computing organizations that support BABAR. The collaborating institutions wish to thank SLAC for its support and the kind hospitality extended to them. This work is supported by the US Department of Energy and National Science Foundation, the Natural Sciences and Engineering Research Council (Canada), the Commissariat à l'Energie Atomique and Institut National de Physique Nucléaire et de

Physique des Particules (France), the Bundesministerium für Bildung und Forschung and Deutsche Forschungsgemeinschaft (Germany), the Istituto Nazionale di Fisica Nucleare (Italy), the Foundation for Fundamental Research on Matter (The Netherlands), the Research Council of Norway, the Ministry of Science and Technology of the Russian Federation, Ministerio de Educación y Ciencia (Spain), and the Science and Technology Facilities Council (United Kingdom). Individuals have received support from the Marie-Curie IEF program (European Union) and the A. P. Sloan Foundation.

* Deceased

† Now at Tel Aviv University, Tel Aviv, 69978, Israel

‡ Also with Università di Perugia, Dipartimento di Fisica, Perugia, Italy

§ Also with Università della Basilicata, Potenza, Italy

¶ Also with Universitat de Barcelona, Facultat de Física, Departament ECM, E-08028 Barcelona, Spain

- [1] Particle Data Group, W.-M. Yao *et al.*, J. Phys. G **33**, 1 (2006).
- [2] Charge conjugated modes are implied throughout the paper.
- [3] From the value reported in [1] rescaled using the new world average for $\mathcal{B}(\eta_c \rightarrow K\bar{K}\pi)$, again from [1].
- [4] Belle Collaboration, F. Fang *et al.*, Phys. Rev. D **74**, 012007 (2006).
- [5] CLEO Collaboration, P. Rubin *et al.*, Phys. Rev. D **72**, 092004 (2005).
- [6] E835 Collaboration, M. Andreotti *et al.*, Phys. Rev. D **72**, 032001 (2005).
- [7] G.T. Bodwin, E. Braaten and G.P. Lepage, Phys. Rev. D **51**, 1125 (1995).
- [8] BABAR Collaboration, B. Aubert *et al.*, Nucl. Instrum. Methods **A479**, 1 (2002).
- [9] S. Agostinelli *et al.*, Nucl. Instrum. Methods **A506**, 250 (2003).
- [10] G. C. Fox and S. Wolfram, Phys. Rev. Lett. **41**, 1581 (1978).
- [11] ARGUS Collaboration, H. Albrecht *et al.*, Z. Phys. C **48**, 543 (1990).
- [12] In the Monte Carlo events, the h_c meson is simulated with a 1 MeV/ c^2 total width.
- [13] BABAR Collaboration, B. Aubert *et al.*, Phys. Rev. Lett. **92**, 142002 (2004).
- [14] BABAR Collaboration, B. Aubert *et al.*, Phys. Rev. Lett. **94**, 171801 (2005).